Time–Temperature-Transformation (TTT) Diagram of the Isothermal Crosslinking of an Epoxy/Amine System: Curing Kinetics and Chemorheology

E. Mounif, V. Bellenger, A. Tcharkhtchi

LIM, ENSAM 151 Bd de l'Hôpital 75013 Paris

Received 27 October 2006; accepted 30 March 2007
DOI 10.1002/app.26612
Published online 27 February 2008 in Wiley InterScience (www.interscience.wiley.com).

ABSTRACT: Rotational molding is a new process for thermosets, few research works have been done on this subject. The goal of this study is to determine the optimal conditions (time, temperature, viscosity, etc) of this process for an epoxy-amine system. The thermal and rheological analysis help us to investigate the vitrification and the gelation of the reactive system (DGEBA-DETDA) and to draw the TTT diagram. We have completed this diagram by adding the isoviscosity curves to determine the available domain for rotational molding. © 2008 Wiley Periodicals, Inc. J Appl Polym Sci 108: 2908–2916, 2008

Key words: epoxy resin; TTT diagram; vitrification; gelation; rotational molding

INTRODUCTION

Rotational molding of reactive systems such as epoxy amine thermosets[1] has been the subject of recent work[2–4] because it presents an attractive alternative to the use of thermoplastic powders in the aim of optimizing cycle times thanks to gelation and opening a new domain of applications. The viscosity variation is the main phenomenon, which affects the cycle time of rotational molding. The evolution of the viscosity is highly dependent on the increase of the molecular weights and the structure evolution of the reactive system during an isothermal cure. Understanding this structure evolution allows us to predict the evolution of the viscosity. Until now, there are no general kinetic schemes universally accepted[5] for the crosslinking of epoxy amine systems. In the case of aromatic amine hardeners, the substitution effect[6,7] (i.e., the formed secondary amine are less reactive than primary amine groups) delays the crosslinking and the formation of the gel. The first formed oligomers will be linear with a few branches which decreases the viscosity comparing with the linear oligomers of the same molecular weight. The most important processing event of a reactive system is the formation of a gel which is a three dimensional, infusible, and insoluble network. The gel time is a critical point for thermosets processing because the system will not flow any more, and the shape of the part will be fixed. Depending on the final application, the conversion ratio can be increased in a later post cure. Many criteria are considered by authors to characterize the gel point (G' and G'' curves intersection, the point for which tan δ is independent of frequency, the divergence point of viscosity and so on...[8]). However, in the case of the rotational molding the processing must be finished before the gel point and the processing has a maximum limit of viscosity η_{max} after which the system has a solid rotation.

Another important property of polymeric materials is the glass transition temperature T_g. The evolution of this property can be linked directly to the conversion ratio $T_g = f(x)$ via Di-Benedetto's equation.[9] Kinetics investigation of chemical reactions [$x = f(t)$] allows us to determine the vitrification curve $T_g = f(t)$ for an isothermal cure.

In this article we tried to define the optimal conditions of rotational molding of an epoxy-amine system, by building up the well-known time-temperature transformation-diagram (TTT),[10–12] and by determining the kinetics parameters, which control the crosslinking process.

Background

Isothermal kinetics

Scheme 1 displays the general accepted mechanism[13] which was first published by Smith[14] and later by Horie and Hiura[15] for the crosslinking of an epoxy prepolymer by an amine hardener. It proposes mainly two ways (catalytic and noncatalytic) of ring

Correspondence to: V. Bellenger (veronique.bellenger@paris.ensam.fr).

Journal of Applied Polymer Science, Vol. 108, 2908–2916 (2008)

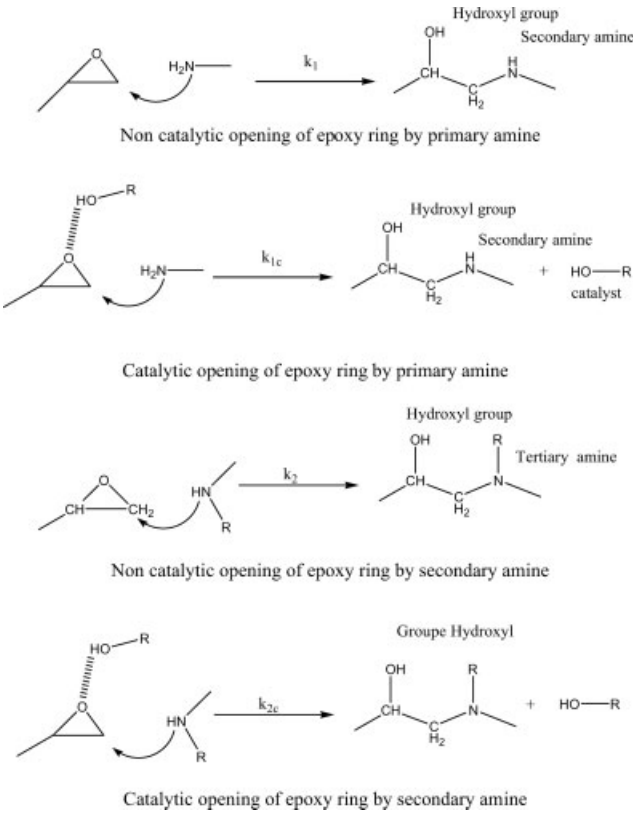

Scheme 1 Curing mechanism of an epoxy prepolymer crosslinked by a diamine.

opening of the epoxy groups. The activation of the ring opening of epoxy is achieved by proton donors especially the produced hydroxyl groups. Both hydroxyl and primary amine groups can catalyze the reaction via the formation of complexes like (E-OH) and (E-A1). We considered only the build-up of epoxy-hydroxyl complexes, which has the main participation in the catalytic mechanism.[16–18] This activation can be achieved by other hydrogen donors or impurities like HX.

Etherification or homopolymerization (Scheme 2) can also occur at high crosslinking temperatures. It can be catalyzed by the presence of tertiary amine groups and when the epoxy is in excess,[19] especially when the epoxy structure contains already tertiary amine groups like tetraglycidyl diamino diphenyl methane (TGDDM) or *N,N*-diglycidyl aniline (DGA).[20] The importance of the etherification depends also on the basicity of the used amine, for instance, in the case of the 4,4′-methylene bis(3-chloro-2,6-diethylaniline) (MCDEA) hardener, the weak basicity of MCEDA makes the etherification a competitive reaction.[21]

The etherification can be neglected in our case, because the DGEBA is not in excess, the structure of DGEBA does not contain any tertiary amine groups and finally crosslinking does not occur at high temperature. The differential equation system controlling the concentration variation of reactive species is:

$$\frac{d[\mathrm{E}]}{dt} = -k_1[\mathrm{A}_1][\mathrm{E}] - k_2[\mathrm{E}][\mathrm{A}_2] \quad (1)$$

$$\frac{d[\mathrm{A}_1]}{dt} = -k_1[\mathrm{E}][\mathrm{A}_1] - k_{1c}K[\mathrm{A}_1][\mathrm{E}][\mathrm{OH}] \quad (2)$$

$$\frac{d[\mathrm{A}_2]}{dt} = k_1[\mathrm{E}][\mathrm{A}_1] + k_{1c}K[\mathrm{A}_1][\mathrm{E}][\mathrm{OH}] - k_2[\mathrm{E}][\mathrm{A}_2] - k_{2c}K[\mathrm{A}_2][\mathrm{E}][\mathrm{OH}] \quad (3)$$

$$\frac{d[\mathrm{OH}]}{dt} = k_1[\mathrm{E}][\mathrm{A}_1] + k_2[\mathrm{E}][\mathrm{A}_2] + 2k_{1c}K[\mathrm{A}_1][\mathrm{E}][\mathrm{OH}] + 2k_{2c}K[\mathrm{A}_2][\mathrm{E}][\mathrm{OH}] \quad (4)$$

$$\frac{d[\mathrm{EOH}]}{dt} = -k_{1c}K[\mathrm{A}_1][\mathrm{E}][\mathrm{OH}] - k_{2c}K[\mathrm{E}][\mathrm{A}_2][\mathrm{OH}] \quad (5)$$

where $[A_1]$, $[A_2]$, [E], [OH], and [EOH] are respectively, the concentrations of primary amine, secondary amine, epoxy, hydroxyl, and activated epoxy groups. The buid-up of an epoxy-hydroxyl complex was considered as a rapid equilibrium compared with other steps of the mechanism and in this case we note the product $k_{ic}K$ as k_{ic}.

The last differential equations system can be modified to take into account the effect of evaporation of monomers on the kinetic of crosslinking,[22] but we think that the evaporation may be neglected when the crosslinking is achieved in a closed crucible (DSC) or quartz cells (FTIR). For crosslinking temperature close to glass transition temperature, the process is controlled by the diffusion[23–26] due to the reduced mobility of reactants in the reactive system. But when the crosslinking temperature (T_{iso}) is 30°C higher than the glass transition (T_g), the effect of the diffusion on the crosslinking mechanism can be neglected.

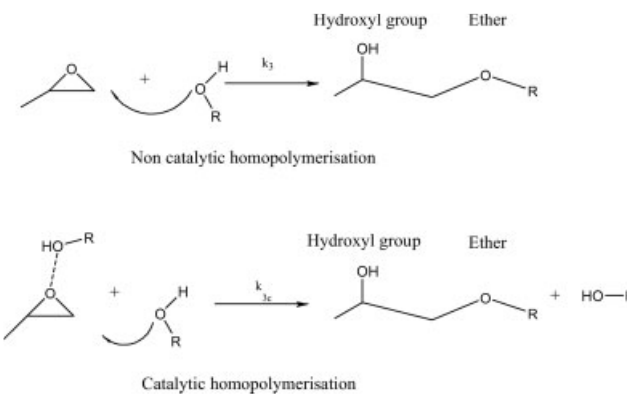

Scheme 2 Mechanism of etherification.

Determination of the chemical kinetic constants

In phenomenological or empirical models, parameters have not necessarily physical meanings. In this research, our aim is to obtain the best parameters for the proposed mechanism which can describe elementary steps taking place and explain the observed experimental results.

The numeric integration of the last differential equation system [eqs. (1)–(5)] is achieved using homemade Matlab programming code based on 4th order semi-implicit Runge–Kutta method.[27] To get the best fit for the primary amine and epoxy group conversion ratios, we have started with an initial estimate of kinetics parameters (Table I) and then a constrained optimization process based on the direct search method (Nelder–Mead Simplex Method[28]) is used to get the best set of parameters. We support the hypothesis that relative reactivity ratio of secondary amines to primary amines, via noncatalytic way ($r = k_2/k_1$) is equal to the catalytic one ($r_c = k_{2c}/k_{1c}$). This ratio is equal to 0.5 for equal reactivities (Table I) of the primary (always interfered as 2 × N—H) and secondary amine (—NRH) groups. Table II contains the initial concentration of different reactive functions.

TABLE I
Initial Estimate and Intervals for the Kinetic Parameters

Kinetic parameter	Initial estimate	Minimum accepted value	Maximum accepted value
k_1 (kg mol^{-1} min^{-1})	0.1	10^{-8}	1
k_{1c} (kg^2 mol^{-2} min^{-1})	0.1	10^{-8}	1
r	0.25	10^{-8}	0.5

TABLE II
Initial Concentrations of Different Functional Groups

	$[E]_0$	$[A_1]_0$	$[A_2]_0$	$[A_3]_0$	$[OH]_0$
Concentration (mol kg^{-1})	4.36	2.24	0	0	0.134

EXPERIMENTAL

Materials

Diglycidyl ether of bisphenol A (DGEBA) with an epoxy equivalent weight of 178 g mol^{-1}, from Fluka is used. Diethyl toluene diamine (DETDA) or Ethacure100 from Safic Alcan exists as a mixture of 2,4 and 2,6 isomers with an N—H equivalent mass of 45 g mol^{-1} and is added as a hardener for epoxy resin. Scheme 3 represents the structures of both components. To prepare the thermoset system, hardener is added to DGEBA in stoichiometric ratio. To obtain a homogenous mixture, the components are mixed at 55°C in an oil bath and degassed under vacuum for 20 min at 40°C.

Methods

Rheological analysis

Rheological properties are measured using an ARES Rheometer from TA instrument equipped with parallel plates with a 0.5–1 mm spacing and a 50-mm diameter. The reactive mixture is added quickly on the preheated plate and a time sweep is started when the temperature equilibrium was reached again. A time ramp at a multifrequency mode is used to determine the gel time considering the loss factor independence of frequency as a criterion of gel point.

Thermal analysis

The cure of investigated systems is studied by means of a differential scanning calorimeter DSC-Q10 from TA instruments, using aluminum hermetic crucibles. The DSC is calibrated in enthalpy and temperature scales by using a high purity indium sample.

Isothermal crosslinking is achieved by three ways:

a. One sample is placed in the preheated DSC cell, and time scan is started when the temperature equilibrium was regained until the base line is reached again.
b. Interrupted crosslinking was achieved *in situ* in the DSC cell in sealed aluminum crucibles. Crosslinking is quenched by a rapid cooling when the desired crosslinking time is reached.
c. Isothermal crosslinking of the reactive system was achieved also in a steel beaker heated by an oil bath under mechanical stirring, samples were taken at different times and quenched by cooling in an ice bath.

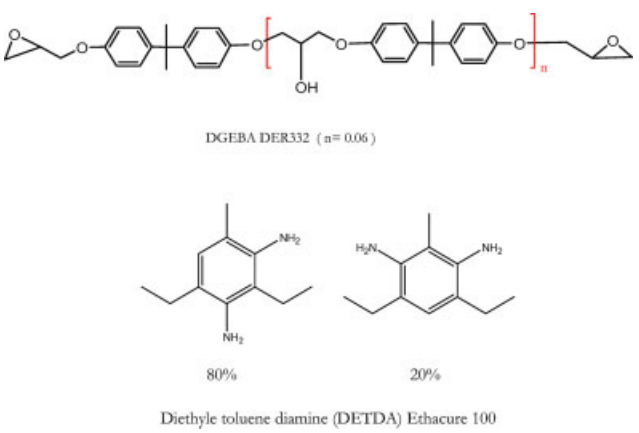

Scheme 3 Chemical structures of prepolymer and hardener. [Color figure can be viewed in the online issue, which is available at www.interscience.wiley.com.]

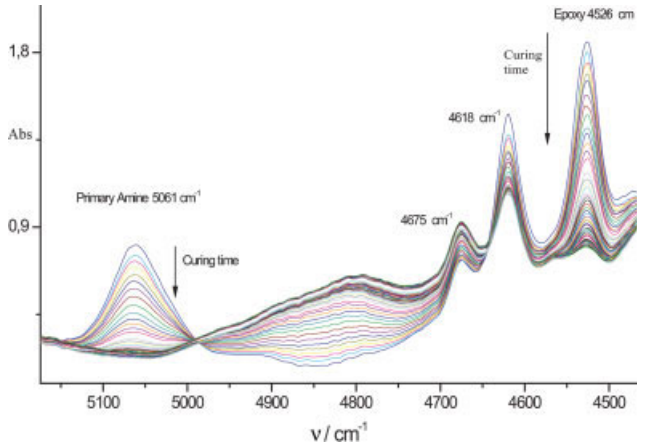

Figure 1 NIR spectrum of the isothermal crosslinking of the reactive system of DGEBA-DETDA. [Color figure can be viewed in the online issue, which is available at www.interscience.wiley.com.]

Running integral of the Universal analysis software (from TA instrument) was used to get the conversion ratio in the first case (a) and a dynamic scan (5°C min C^{-1}) of partly cured samples was done to measure the residual enthalpy and glass transition temperature T_g (b and c).

Working at high heating rates shifts the reaction to higher temperature and in this case it would not be easy to neglect side reactions. The choice of the heating rate was optimized to get a good estimate of glass transition temperature.

The total heat of reaction, ΔH_{tot}, is estimated from nonisothermal experiments. In these experiments, sample is heated from initial temperature T_{ini} to final temperature T_f, with linear heating rates of 2, 5, 7, and 10°C min^{-1}. ΔH_{tot} is calculated by drawing a linear baseline and integrating the area under the peak. The heat of isothermal reaction is estimated by extrapolating the final baseline. Dynamic DSC experiments are also performed to determine the glass transition temperature, of an uncured T_{g0}, and completely cured material $T_{g\infty}$. The glass transition temperature is taken as the inflection point of the second order endothermic transition.

Near infra red (NIR) spectroscopy

Fourier transform NIR spectroscopy is performed using Bruker IFS28 spectrophotometer, equipped with a Globar source, KBr beam splitter, and DTGS detector. All spectra (Fig. 1) were collected in the near infra red domain (7500–4000 cm^{-1}) at a 4 cm^{-1} resolution and 32 scans per sample. For thermal control, a temperature controller is used (Specac). The reactive mixture is injected with a syringe in the cell (Quartz with 2-mm pathlength) when the controller showed the programmed temperature.

When samples with various thicknesses are analyzed, a reference band has to be considered. Phenyl groups absorption bands (4623, 4681, 4065 cm^{-1}) are widely used in the literature.[29] In our case the same cell is used for all experiments; therefore we applied the simple equation: $x_{NIR} = 1 - \frac{A_1}{A_0}$, to quantify the epoxy conversion ratio; A_t/A_0 is the ratio of actual area of peak with respect to initial one.

RESULTS AND DISCUSSION

Effect of various crosslinking conditions

Figure 2 shows the results of thermal analysis of the three last crosslinking ways. Conversion ratio versus cure time curves in isothermal curing conditions are obtained by normalizing the integral heat flow curves with respect to the total enthalpy of reaction of fully reacted samples. A good agreement is noticed between experimental results of various types of curing conditions. The use of running integral for one sample isothermal curing allows determining quickly the conversion ratio versus the cure time or the heat flow versus the conversion ratio. The heat flow is supposed to be proportional to reaction rate $\frac{dQ}{dt} = \frac{1}{\Delta H_{tot}} \frac{dx}{dt}$, the extrapolation of the baseline to $t = 0$ min is more difficult at high temperature (Fig. 3) due to the difficult stabilization of temperature in the sample at the beginning of the experiment.

The average reaction enthalpy of the equimolar mixtures (ΔH_{tot} = 92 J/epoxy equivalent) was in agreement with those reported in literature[30–32] for similar reactive systems. It should be noticed that in our case, conversion ratios determined by DSC and

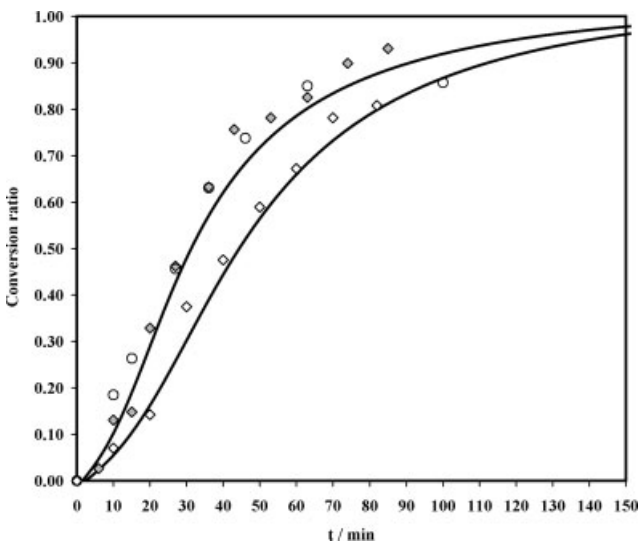

Figure 2 Comparison between different kinds of curing conditions (T = 140°C, (◆): Sample Crosslinked in oil bath (○): Sample Crosslinked in the DSC cell, (—): running integral) (T = 130°C (◇): Sample Crosslinked in oil bath, (—): running integral).

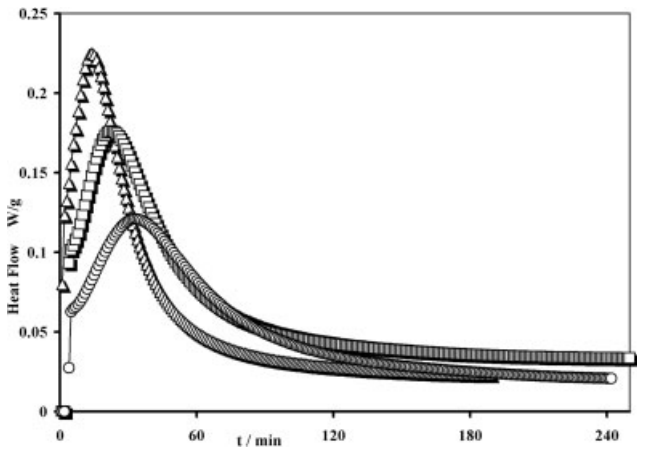

Figure 3 Heat flow for different conditions of isothermal cure 130°C (○), 140°C (□), and 150°C (△).

NIR spectroscopy (Fig. 4) are no more comparable after the gel point. In fact the sharp increase of the viscosity at the gel point and the consumption of reactive species lower the reaction rate. Concerning, the DSC measurement, the heat flow decreases and heat dissipation becomes more difficult to detect. When one considers conversion ratio obtained by NIR spectroscopy (x_{NIR}), the chemical absorbance also decreases and integrating the absorption band was not easy due to the weak measured energy; so both methods of characterization become less efficient. We were interested in characterizing the reactive system before gelation, where the process is controlled by chemical kinetics.

Kinetics parameters

A good agreement is noticed between the numeric solution and the experimental data (Figs. 5 and 6)

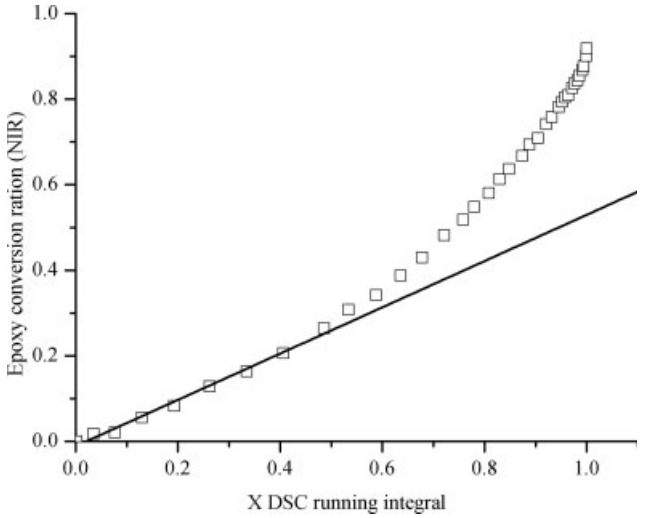

Figure 4 Comparison between conversion ratios of epoxy groups obtained by DSC and NIR methods. Experimental results (□) and linear fit (—).

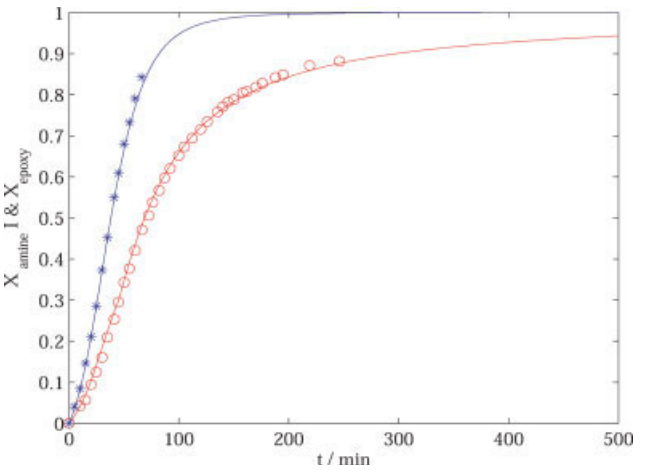

Figure 5 Conversion ratio of primary amine (*) and epoxy (○) groups during a cure at 130°C and Matlab numeric solution (—). [Color figure can be viewed in the online issue, which is available at www.interscience.wiley.com.]

for the cure temperatures $T = 130$°C and $T = 140$°C. Table III shows the numeric values of the catalytic and noncatalytic parameters, obtained by the last optimization. Obviously, the reaction occurs mainly by a catalytic mechanism and the contribution of a noncatalytic mechanism can be neglected.

The reactivity ratio increases with temperature, which means that primary amines are still more reactive at high temperature than secondary ones. Supposing that all kinetics parameters follow Arhennius Law, $k = A \exp(E_a/RT)$, one can estimate (Table IV) the corresponding activation energies (E_a) and the pre-exponential factors (A). As expected, catalytic activation energies are lower than those of noncatalytic reactions and higher than those obtained by

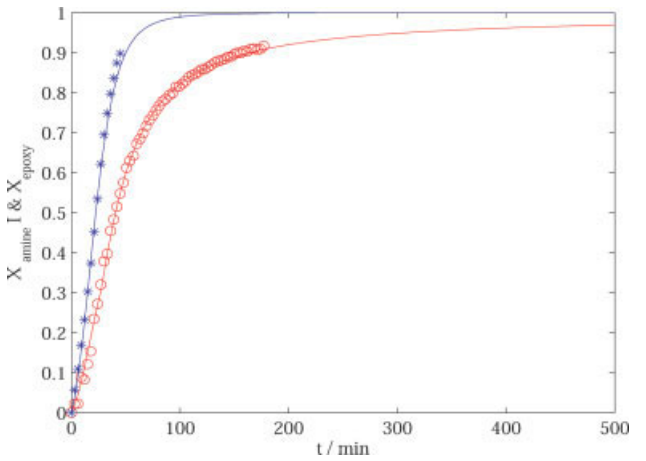

Figure 6 Conversion ratio of primary amine (*) and epoxy (○) groups during a cure at 140°C and Matlab numeric solution (—). [Color figure can be viewed in the online issue, which is available at www.interscience.wiley.com.]

TABLE III
Kinetics Parameters of the Crosslinking Reaction Between DGEBA and DETDA at 130°C and 140°C Cure Temperature

	130°C	140°C
k_1 (kg mol^{-1} min^{-1})	1.6×10^{-4}	7.6×10^{-4}
k_2 (kg mol^{-1} min^{-1})	4.8×10^{-5}	2.6×10^{-4}
k_{1c} (kg^2 mol^{-2} min^{-1})	7.0×10^{-3}	1.1×10^{-2}
k_{2c} (kg^2 mol^{-2} min^{-1})	2.0×10^{-3}	3.8×10^{-3}
r	0.29	0.35

Uhlherr and coworkers[6] who considered only the catalytic mechanism.

Vitrification

When the increasing T_g value approaches the isothermal cure temperature, the molecular mobility is strongly reduced and the reaction becomes diffusion controlled and eventually breaks off. The variation of the glass transition temperature (T_g) versus the crosslinking ratio, determined by DSC (x-DSC) is found to follow Di Benedetto equation:

$$T_g = T_{g0} + \frac{\lambda(T_{g\infty} - T_{g0})x}{1 - (1 - \lambda)x},$$

With $\lambda = (\Delta C_p^{\infty}/\Delta C_p^{0})$ heat capacity change ratio. It is measured through the glass transition for uncured and fully cured system by DSC. The measured value of $\lambda = 0.27$ is different from that found by O'Brien and White[7] (i.e., $\lambda = 0.392$) but it is in good agreement with the best fit obtained parameter ($\lambda = 0.28$) (Fig. 7). Until the gel point, the glass transition temperature T_g is smaller than the curing temperature T_{cure}, which means that the gelation takes place before the vitrification. The curve of $T_g = f(x)$ is a good tool to get the time to vitrification and to establish finally the vitrification curve (see TTT diagram).

Rheological analysis

The measurement of the rheological properties is done using auto strain mode. The strain increases at the beginning of the crosslinking till its maximum allowed value and decreases at gel point to avoid the breaking of the formed network (Fig. 8). To verify the linear viscoelasticity of the system and to see the influence of this mode on the rheological properties, we have carried out a dynamic strain sweeps

TABLE IV
Activation Energies as Estimated from NIR Measurement for Catalytic and Noncatalytic Mechanisms

	k_1	k_2	k_{1c}	k_{2c}
ln A)	55	61	13	19
E_a (kJ mol^{-1})	213	237	61	85

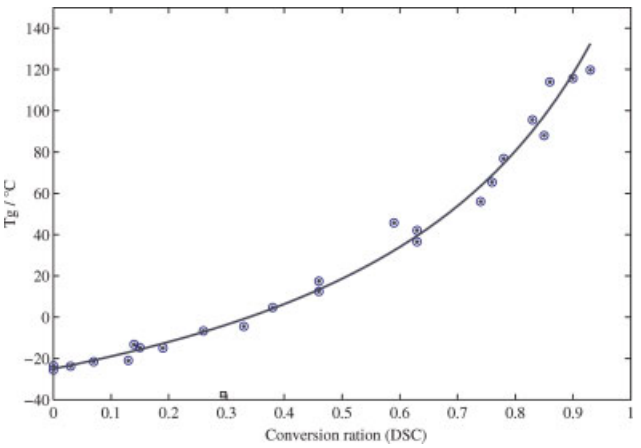

Figure 7 Glass transition temperature as a function of DSC conversion ratio. Experimental results (Θ) and Di Benedetto fit (—). [Color figure can be viewed in the online issue, which is available at www.interscience.wiley.com.]

for partly cured sample (Figs. 9 and 10). The same value for the pregel viscosity is founded and values diverge only in the vicinity of the gel point because of nonlinear effects of the built up network. The rheological behavior of different epoxy-amine reactive systems in terms of scaling laws is studied in details in literature.[33–35] In our case we focused our interest on two essential phenomena: gelation and vitrification.

Gelation

The gel point was obtained by considering the time to reach a value independent of the frequency (Fig. 11), using multi-frequency experiments. One must

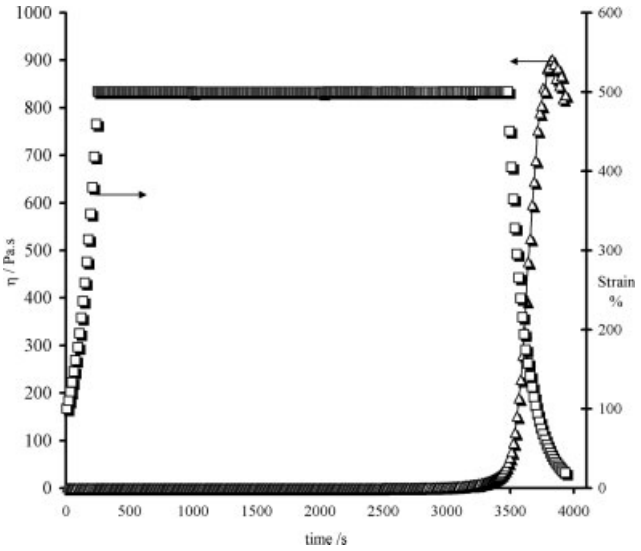

Figure 8 Experimental curves of the real part of dynamic viscosity η' (△), and strain $\dot{\gamma}$ (□) versus time during isothermal crosslinking of the DGEBA-DETDA reactive system.

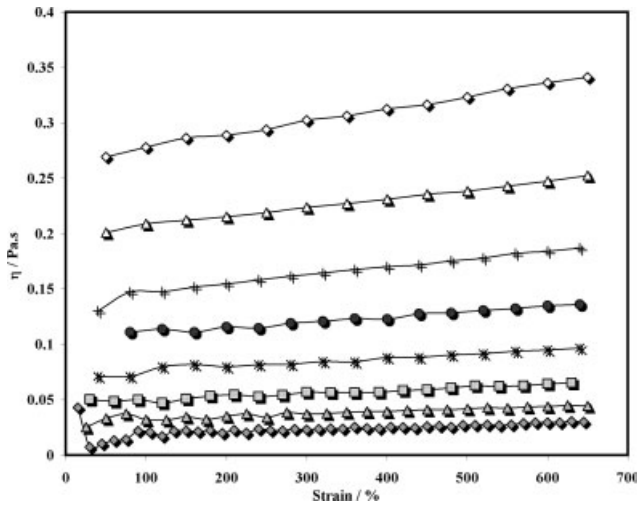

Figure 9 Experimental curves of the real part of dynamic viscosity (η′) measured by strain sweeps at 130°C. Each strain sweep was done after different curing times: 10 min (◇), 23 min (◆), 29 min (▲), 33 min (■), 36 min (∗), 39 min (●), 41 min (+), 44 min (△), and 46 min (◇).

pay attention to the minimal frequency value (f_{min}) which can be used; this value depends on the curing temperature (T_{cure}). In fact, at every frequency, the reaction rate has to be low during measurements. We considered the condition proposed by Izuka et al.[36]: $(1/G^*)\ (\partial G^*/\partial t)\ (2\pi/\omega) < 0.1$. In our case, the gel times measured by different rheological criteria are almost the same. The gel times of the DGEBA-DETDA system for several isothermal conditions are summarized in Table V. Measuring the gel time at higher temperatures is inaccurate because the temperature stabilization time is considerable compared

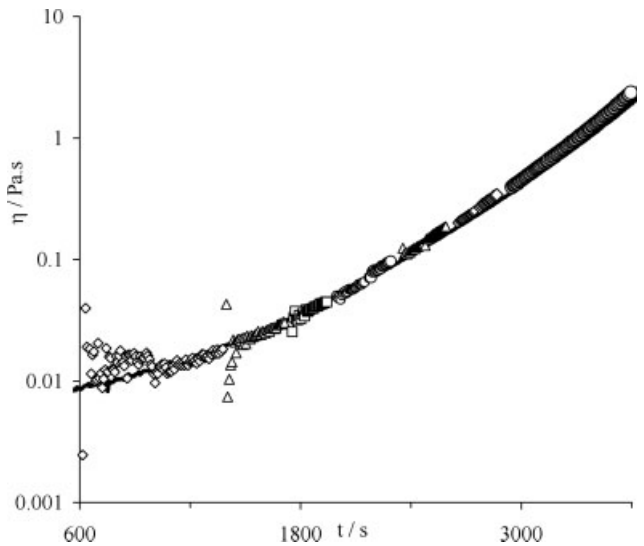

Figure 10 Dynamic viscosity of reactive system measured by strain sweeps at various times of the crosslinking. The different parts of Figure 9 were connected considering the elapsed curing time.

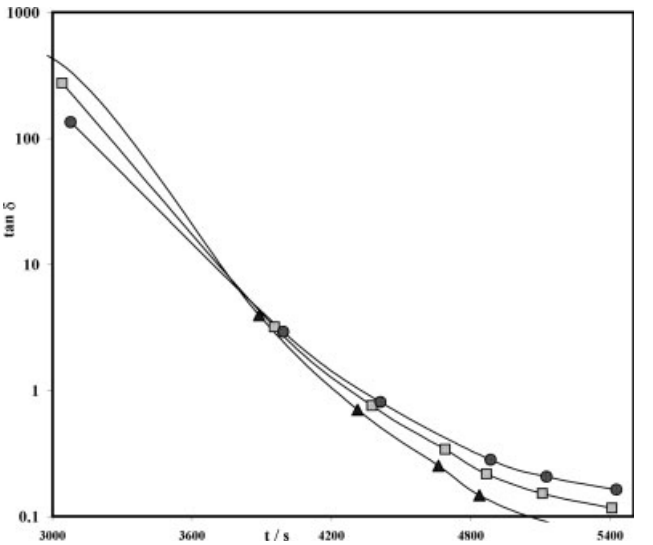

Figure 11 Loss factor (tan δ) versus time for DGEBA-DETDA system cured at 130°C, measured at three frequencies 2 Hz (▲), 5 Hz (■), and 10 Hz (●).

with the gel time. The Arrhenius plot of the gel times listed in the Table V is shown in Figure 12.

$$t_{gel} = Ae^{\frac{-E}{RT}}$$

where E_a is the activation energy, T is the absolute temperature of reaction, and R is the universal gas constant. The activation energy of the reaction is equal to 60 kJ mol^{-1}, which is a reasonable value compared with the one of bisphenol A type epoxy resin and aromatic amine compounds.[37] When comparing the gel point as measured by the parallel plate rheometry for different temperatures, we found that the critical conversion ratio as measured by DSC was about $x = 0.70$ which is different from the theoretic critical value calculated by Flory relationship. In the case of our system [tetra functional hardener (diamine) +(bi functional epoxy)], the calculated critical value x_{gel} is equal to 0.58. The main reason for this is the difference in reactivity (substitution effect delays the gel point[38]) between primary and secondary amines groups.

Time-temperature-transformation (TTT) diagram

The Diagram Time-Temperature-Transformation is established experimentally. For each isothermal curing temperature we determined the times it takes to gelation (t_{gel}) and to vitrification. We notice that the vitrification takes place after gelation and the cross-

TABLE V
Gel Times for Different Isothermal Cure Temperatures

Curing temperature (°C)	120	130	135	140	150
Gel time (min)	100	63	46	42	29

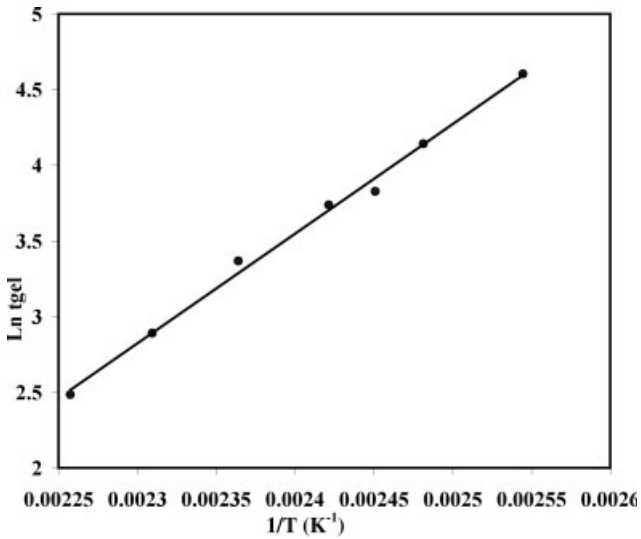

Figure 12 Arhennius plot of gel times.

linking proceeds until gelation (end of polymer flow and polymer processing) without being disturbed by the vitrification phenomenon. We verified the thermal stability of the isothermally formed network by TGA measurement: The onset of thermal degradation is far away from gelation and vitrification times.

In the case of reactive rotational molding, the processing is controlled by the viscosity variation during the crosslinking. For that reason, we overlay the curve of isoviscosity on the TTT diagram (Fig. 13). The suitable interval of viscosity for rotational molding depends on other processing parameters[39] like the mold dimensions and the rotation rate to achieve a stationary stable flow (rimming flow) before the gelation.

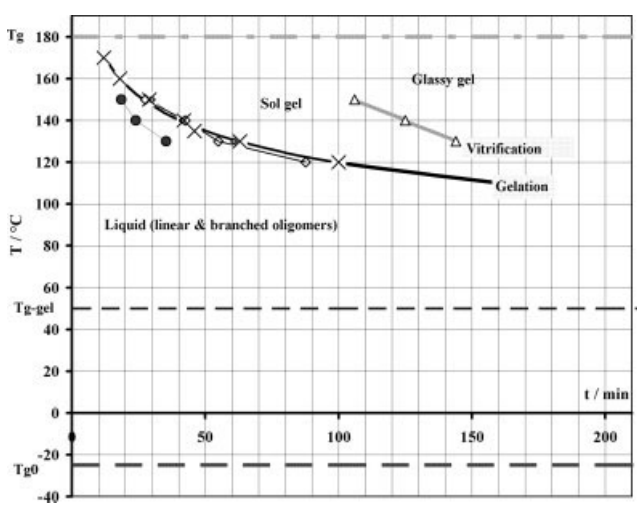

Figure 13 Time-Temperature-Transformation diagram with isoviscosity curves 500 (◆), 0.1 (●), 10 (◇) Pa s. Vitrification (△), gelation (×).

CONCLUSIONS

The kinetic parameters of a DGEBA-DETDA thermoset crosslinking are identified. A catalytic and noncatalytic mechanism is considered for modeling the evolution of epoxy and amine conversion ratios versus time. The gelation of the reactive system is studied in isothermal curing conditions. The gel time is determined as a congruency in the time evolution of the tan δ curves obtained at different frequencies. The variation of glass transition temperature versus conversion ratio is found to be in a good agreement with Di Benedetto equation. Finally the TTT diagram is established coupling the thermal and rheological measurements.

Our next work is to couple these interfered phenomena: chemical reaction and heat conduction to predict the flow of the reactive fluid.

References

1. Harkin-Jones, E.; Crawford, R. Adv Polym Technol 1996, 15, 71.
2. Corrigan, N.; Harkin-Jones, E.; Brown, E.; Coates, P. D.; Crawford, R. J. Plast Rubber Compos 2004, 33, 37.
3. Marcilla, A.; García, J. C.; Ruiz, R.; Sánchez, S.; Vargas, C.; Pita, L.; Beltrán, M. I. Int Polym Process 2005, 20, 47.
4. Tcharkhtchi, A.; Verdu, J. Adv Eng Mater 2004, 6, 983.
5. Pascault, J. P.; Sautereau, H.; Verdu, J.; Williams, R. In Thermosetting Polymer; Marcel Dekker: New York, 2002.
6. Liu, H.; Uhlherr, A.; Varley, R. J.; Bannister, M. K. J Polym Sci Part A: Polym Chem 2004, 42, 3143.
7. Miller, D. R.; Macosko, C. W. Macromolecules 1980, 13, 1063.
8. Halley, P. J.; Mackay, M. E.; George, G. A. High Perform Polym 1994, 6, 405.
9. Pascault, J. P.; Williams, R. J. J. S. Polym Bull 1990, 24, 115.
10. Enns, J. B.; Gillham, J. K. J Appl Polym Sci 1983, 28, 2567.
11. De Miranda, M. I. G.; Samios, D. Eur Polym J 1997, 33, 325.
12. Núñez, L.; Fraga, F.; Castro, A.; Núñez, M. R.; Villanueva, M. Polymer (Guildford) 2001, 42, 3581.
13. Blanco, M.; Corcuera, M. A.; Riccardi, C. C.; Mondragon, I. Polymer 2005, 46, 7989.
14. Smith, I. T. Polymer 1961, 2, 95.
15. Horie, K.; Hiura, H. J Polym Sci Part A-1: Polym Chem 1970, 8, 1357.
16. Flammersheim, H. J. Thermochim Acta 1998, 310, 153.
17. Rozenberg, B. A. Epoxy Resins and Composites II; Springer-Verlag: Berlin, 1986; p 113.
18. Mezzenga, R.; Boogh, L.; Månson, J. A. E.; Pettersson, B. Macromolecules 2000, 33, 4373.
19. Vinnik, R. M.; Roznyatovsky, V. A. J Therm Anal Calorim 2003, 74, 29.
20. Matejka, L. Macromolecules 2000, 33, 3611.
21. Ramos, J. A.; Pagani, N.; Riccardi, C. C.; Borrajo, J.; Goyanes, S. N.; Mondragon, I. Polymer 2005, 46, 3323.
22. Paz-Abuin, S.; Pellin, M. P.; Paz-Pazos, M.; Quintela, A. L. Polymer 1997, 38, 3795.
23. Flammersheim, H. J. Opfermann, J. Thermochim Acta 1999, 337, 141.
24. Deng, Y.; Martin, G. C. Macromolecules 1994, 27, 5147.
25. Prolongo, S.; Mikes, F.; Cabanelas, J.; Paz-Abuin, S.; Baselga, J. J Mater Process Technol 2003, 143, 546.
26. Wise, C.; Cook, W.; Goodwin, A. Polymer 1997, 38, 3251.
27. Swier, S.; Assche, G. V.; Mele, B. V. Thermochim Acta 2004, 411, 149.

28. Lagarias, J. C.; Reeds, J. A.; Wright, M. H.; Wright, P. E. SIAM J Optim 1998, 9, 112.
29. Poisson, N.; Lachenal, G.; Sautereau, H. Vib Spectrosc 1996, 12, 237.
30. Naffakh, M.; Dumon, M.; Dupuy, J.; Gérard, J. F. J Appl Polym Sci 2005, 96, 660.
31. O'Brien, D. J.; Mather, P. T.; White, S. R. J Compos Mater 2001, 35, 883.
32. O'Brien, D. J.; White, S. R. Polym Eng Sci 2003, 43, 863.
33. Eloundou, J. P.; Feve, M.; Gerard, J. F.; Harran, D.; Pascault, J. P. Macromolecules 1996, 29, 6907.
34. Eloundou, J. P.; Gerard, J. F.; Harran, D.; Pascault, J. P. Macromolecules 1996, 29, 6917.
35. Eloundou, J. P.; Ayina, O.; Ngamveng, J. N. Eur Polym J 1998, 34, 1331.
36. Izuka, A.; Winter, H. H.; Hashimoto, T. Macromolecules 1994, 27, 6883.
37. Ishii, Y.; Ryan, A. J. Macromolecules 2000, 33, 158.
38. Miller, D. R.; Macosko, C. W. Macromolecules 1980, 13, 1063.
39. Throne, J. L.; Gianchandani, J. Polym Eng Sci 1980, 20, 899.